

# CHAPTER 1

## INTRODUCTION AND LITERATURE REVIEWS

### 1.1 Introduction

Recently, energy has been one of the most important factors in human's life since all countries over the world demand more energy. One of energy is the energy from fossil such as fuel oil, natural gas, and coal. The amount of fuel oil is decreasing every day while the demand of using it is uncontrollable. This leads to environmental problems; thus, it is necessary to help decreasing energy consumption and looking for other new types of energy. Therefore, there are many renewable energy sources that can compensate for the fossil energy.

Solar energy is one of renewable energy that can be used for long-term period, from past up to present, and it is also environmentally friendly (Kalogirou, 2004). Solar energy has been developed to application continuously. One technology of solar energy utilization is solar water heater. Its system is not complicated and interesting, so it becomes the most pervasive technological device used for solar energy exploitation. Besides, solar energy is absorbed in thermal form and concurrently transferred into hot water by a solar collector. For this reason, there are several types of collectors used in solar systems such as flat plate collector, evacuated tube collector and heat pipe collector (Han et al., 2010). The evacuated tube solar collector has high capability to absorb heat, compared with flat plate collector, since it provides the combined effects between highly selective surface coating and absorber surface's vacuum insulation. At low solar radiation rate, the evacuated tube solar collector yield efficiency higher than flat plate collector as the evacuated tubes has small heat losses (Brunold et al., 2007; Jun-feng et al., 2009).

Evacuated tube solar collectors can be classified into three types which are (a) Water-in-glass evacuated tube solar collector (b) U-type or single phase thermosyphon evacuated tube solar collector, and (c) Heat pipe or two-phase

thermosyphon evacuated tube solar collector. For two-phase thermosyphon, it is the equipment with high thermal conductivity which is used for heat transferring. It should be noted that the isothermal level is the principal properties of two-phase thermosyphon for solar applications.

Moreover, two-phase thermosyphon equipment also contains a small amount of working fluid that received from an evaporating-condensing cycle. (Ismail & Abogderah, 1998; Chun et al., 1999). In this cycle, solar heat evaporates the liquid and the vapor moves to the heat sink. After that, it condenses and heat is transferred by latent heat. The condensed fluid will then return to evaporator section of a solar collector, and the process is repeated (Redpath, 2012). The previous work of two-phase thermosyphon is illustrated theoretically and experimentally. Nada et.al (2004) presented the optimal mass flow rate while Azad (2008) presented the optimum ratio of evaporator length to condenser length. It can be said that, the proper thermosyphon dimensions and numbers of evacuated tube will influence thermal efficiency of the solar collector.

In this research, the solar water heater system is developed from the experiment and mathematical models using the thermal resistance method and Finite Difference Method (EFDM). The solar intensity and ambient air temperature data for the system modeling used of Chiang Mai province, Thailand to predict optimal parameters of solar water heater system. The optimal parameters are analyzed by the thermoeconomic and then it is designed, constructed and tested for the prototype of solar water heater system. The results of the mathematical model are verified by the experiment results under the same operating condition. After that, the cumulative heat rate of water is converted to the electric bill for economics analysis compared to the electric hot water.

## **1.2 Literature Review**

Literature review is divided into two parts. The first one reviews the experimental research of solar water heater system while the second one presents the research of the mathematical model validated with the experiment.

### 1.2.1 The experimental research

Abreu and Colle (2004) studied the two-phase thermosyphons for Solar Domestic Hot Water System (SDHWS) which an unusual geometry characterized by a semicircular condenser and a straight evaporator as shown in Figure 1.1. The evaporator length, fill ratio of working fluid, tilt angle of the evaporator and cooling temperature are investigated for various heat flux from 400 to 1200 W/m<sup>2</sup>

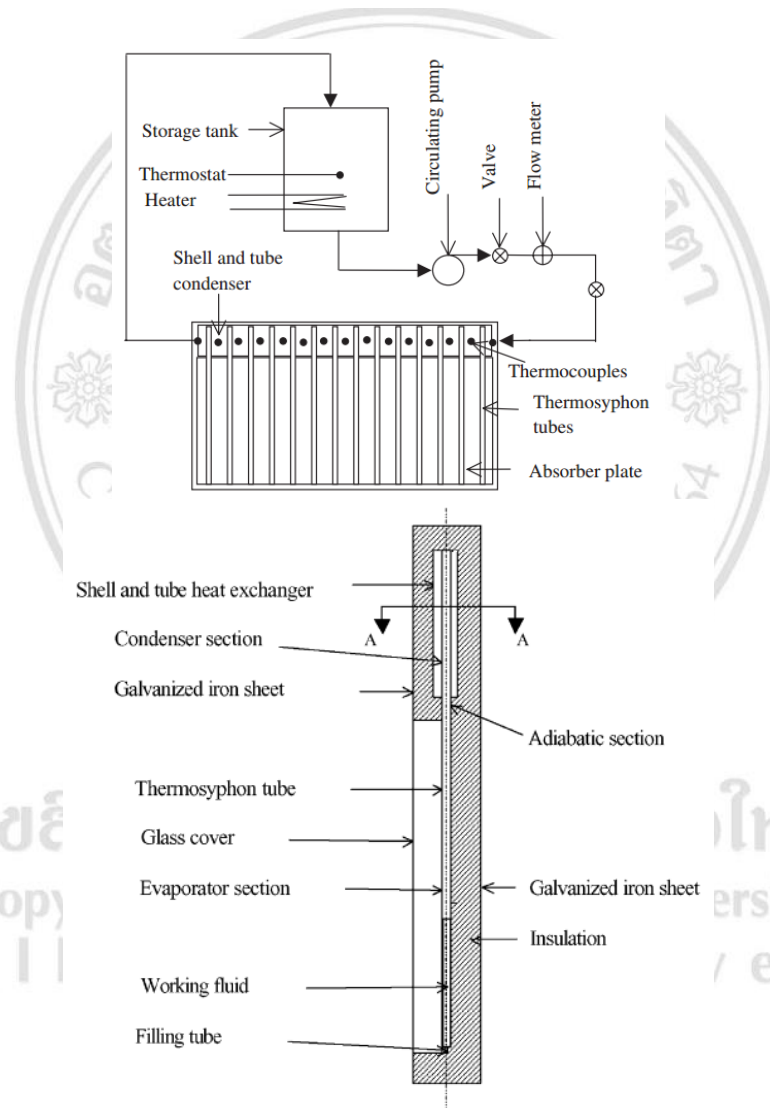


**Figure 1.1** Experimental set up of the two-phase thermosyphon for solar domestic hot water system (Abreu & Colle, 2004)

The evaporator and condenser temperatures are compared. As the tilt angle increases from 30° to 45°, the larger tilt angle and smaller tilt angle is almost the same. The results in the studies, the prototype of the compact SDHWS will be used in the designed and constructed, the obtain results of the system performance will be a similar.

Nada et al. (2004) studied the flat-plate thermosyphon solar collector with a shell and tube heat exchanger. The experimentally is tested under the weather conditions of Cairo, Egypt. A schematic diagram of the experimentally and cross-sectional views of the flat-plate thermosyphon collector is shown in Figure 1.2. The results showed that, the collector efficiency increases by increasing the flow rate from 0.0125 to 0.0292 kg/s, then the collector efficiency decreases with the increase of the flow rate from 0.0292 to 0.0625 kg/s is shown in Figure 1.3.

The maximum collector efficiency occurs at a water flow rate about 0.0292 kg/s. This water flow rate is nearly equal to the ASHRAE standard mass flow rate (mass flow rate =  $0.02A$ , kg/s). As the mass flow rate 0.0292 kg/s, the effect of number of tubes is investigated. It found that, the transient efficiency increases by increasing the number of thermosyphon tubes from 8 to 12 pipes. After that, the number of thermosyphon tubes increases over 12, the transient collector efficiency is the decrease because of the more heat losses.



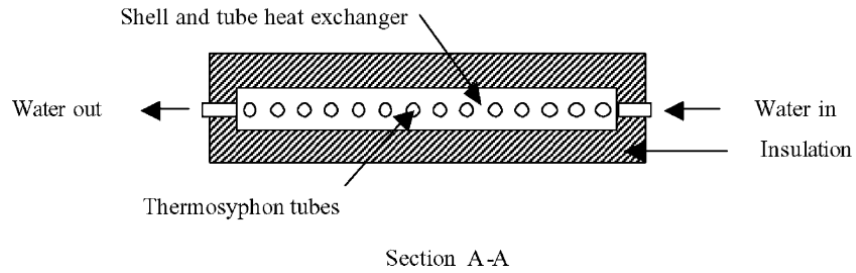


**Figure 1.2** Schematic diagrams of the experimentally components and cross sectional views of the flat-plate thermosyphon collector (Nada et al., 2004)

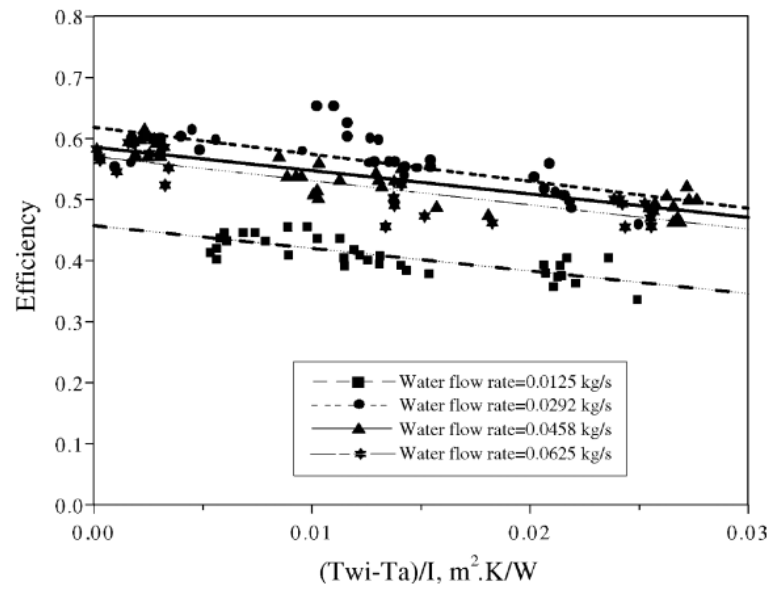


**Figure 1.3** Efficiency of the collector at different water flow rates (Nada et al., 2004)

The thermal performances of the two-phase thermosyphon solar collector using different working fluid are investigated by Mehmet and Hikmet (2005).

Copyright © by Chiang Mai University  
All rights reserved

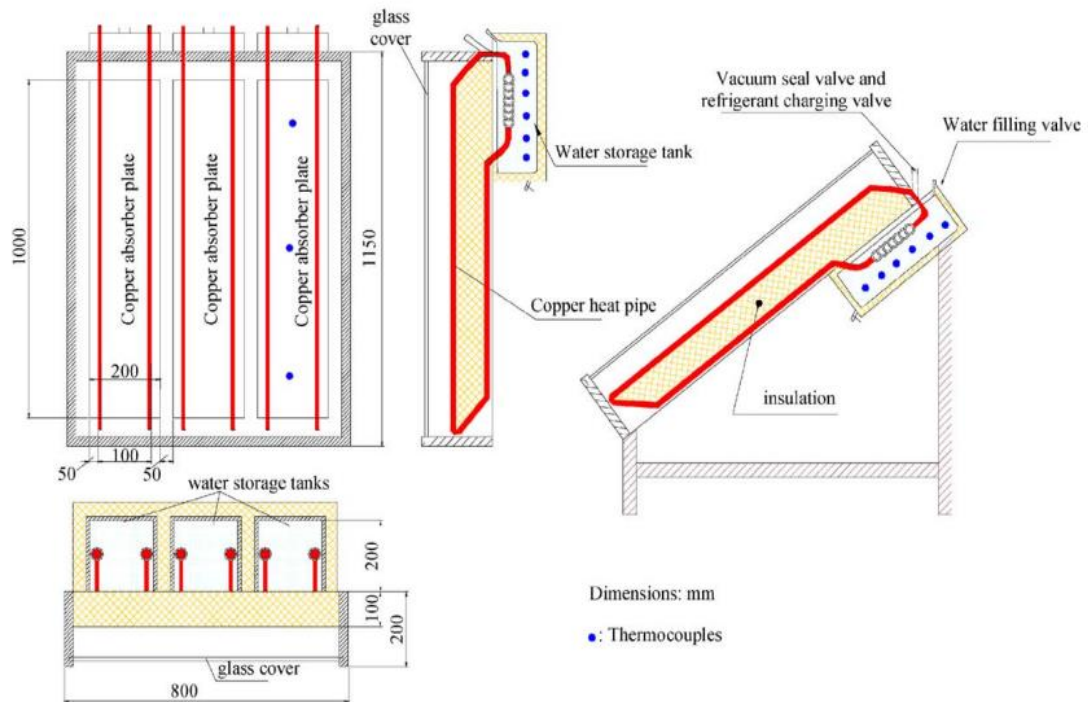


**Figure 1.4** Experimental set-up of two-phase thermosyphon solar water heater

(Mehmet & Hikmet, 2005)

Three identical small solar collector using refrigerants R-134a, R407C, and R410A, are designed and tested side-by-side under weather conditions and load conditions of Elazığ, Turkey as shown in Figure 1.4. Each thermosyphon is filled with 70 g of the refrigerant and the each hot water storage tank volume is set to 10 liter. The results showed that, the daily maximum water temperature changes from 35.5°C to 64.4°C and the maximum collector efficiency varies from 50.86% to 57.13% for R410A. Best efficiency is obtained using R410A because of its higher latent heat, higher thermal conductivity, and lower viscosity.

### 1.2.2 The mathematical model and experiment research

The shapes of absorber tube of evacuated tube solar collector are investigated by numerically and experimentally (Yong & Taebeom, 2006). In the study, four different shapes of the absorber tube are shown in Figure 1.5. In Figure 1.5, Finned tubes (model I), U-tube welded inside a circular fin (model II), U-tube welded on a copper plate (model III), and U-tube welded inside a rectangular duct (model IV).

Model I, the absorber tube are used three diameters with 12.7, 19.05 and 25.4 mm. and the absorber tubes of model II, model III, and model IV are 12.7 mm.

The collectors are divided as 6 cases. Case 1, a copper tube diameter is 12.7 mm for model I. Case 2 and Case 3; copper tubes are 19.05 and 25.4 mm for model I, respectively. Case 4, Case 5, and Case 6 represent model II, model III, and model IV, respectively. The results are shown in Figure 1.6 and Table 1.1

As the incidence angle is lower, the Case V is showed better of the outlet temperature and the efficiency. As the incidence angle increases, the outlet temperature and the model efficiency of Case V promptly decreases. Although the outlet temperature and the model efficiency of Case IV are not greater than Case V when the incidence angle is 0, Case IV is become higher than Case IV as the incidence angle increases because of the performance of model II for Case IV does not depend on the incidence angle. For Case V, the absorber area suddenly decreases as the incidence angle increases due to the shadow due to the circular tube of oneself is throw on the fin area of oneself. Case IV does not have the shadow effect. The center distances of collector on the performance are analyzed for all models. The results shown in Figure 1.7, as the center distance increases are 42, 50, 67, 80, and 90 mm, number of collector tubes decreases and the model III is better performance than the other model at center distance of 42 mm.

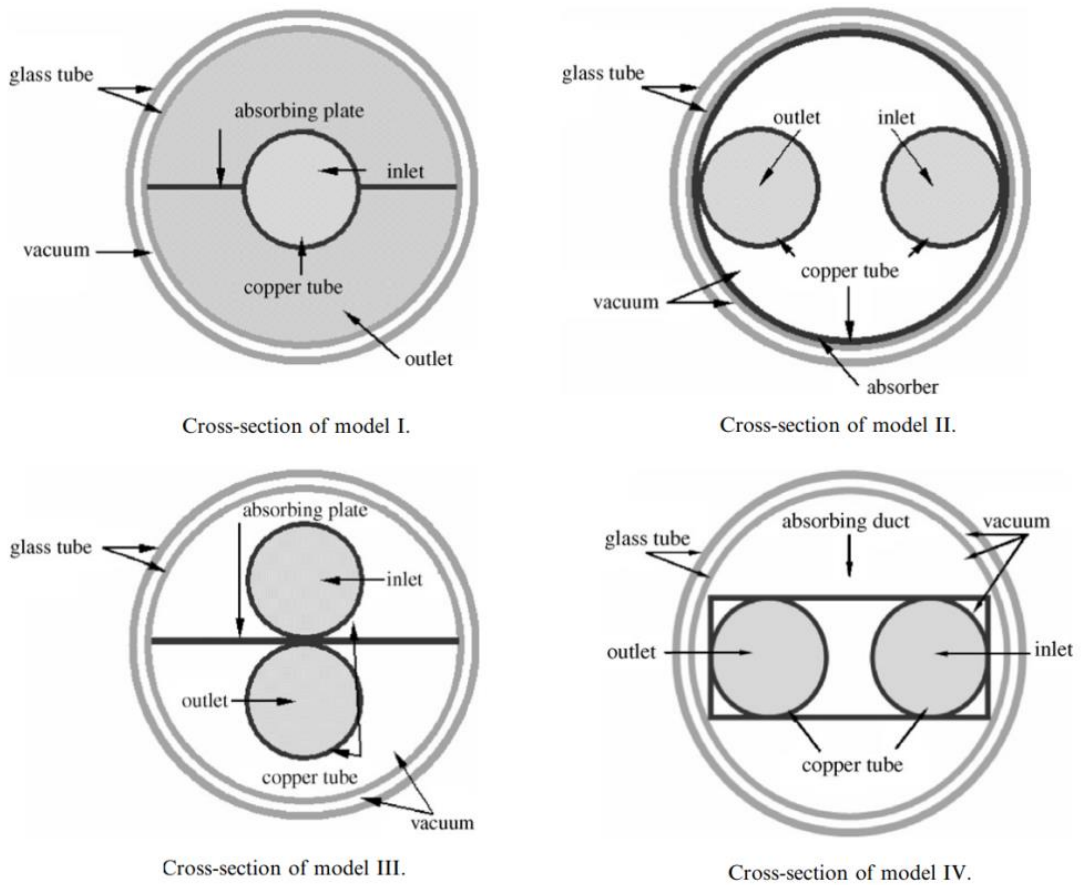


**Figure 1.5** Cross-section of the absorber solar collector (Yong & Taebeom, 2006)

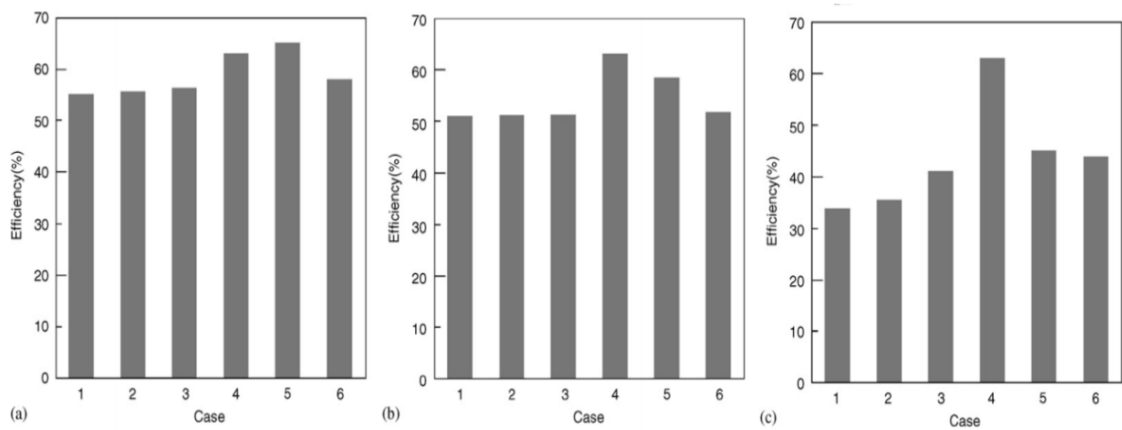


**Figure 1.6** Different configurations of the collector (Yong & Taebeom, 2006)

**Table 1.1** Outlet temperatures and efficiency (Yong & Taebeom, 2006)

Case	Incidence angle = 0°	Incidence angle = 30°	Incidence angle = 60°
------	----------------------	-----------------------	-----------------------



	T (°C)	$\eta$ (%)	T (°C)	$\eta$ (%)	T (°C)	$\eta$ (%)
1	42.9	55.1	41.8	51.1	36.8	33.9
2	43.1	55.8	41.8	51.2	37.3	35.5
3	43.3	56.5	41.9	51.4	38.9	41.2
4	45.3	63.2	45.3	63.2	45.3	63.2
5	45.9	65.2	43.9	58.5	40.1	45.4
6	43.8	58.1	44.9	61.9	39.8	44.0

Budiardjo and Morrison (2008) investigated the water-in-glass evacuated tube solar water heaters are compared to flat plate solar collectors by the experimental and Transient System Simulation (TRNSYS). A water-in-glass of single-ended tubes connected to a storage tank. The heat transfer in collector is natural circulation of water flow passes the single-ended tubes. The flow is driven by the weight difference of hot water in the return pipe and the cold water in the downcomer. A standard Type 45 TRNSYS used for the water-in-glass evacuated tube collector as shown in Figure 1.8.

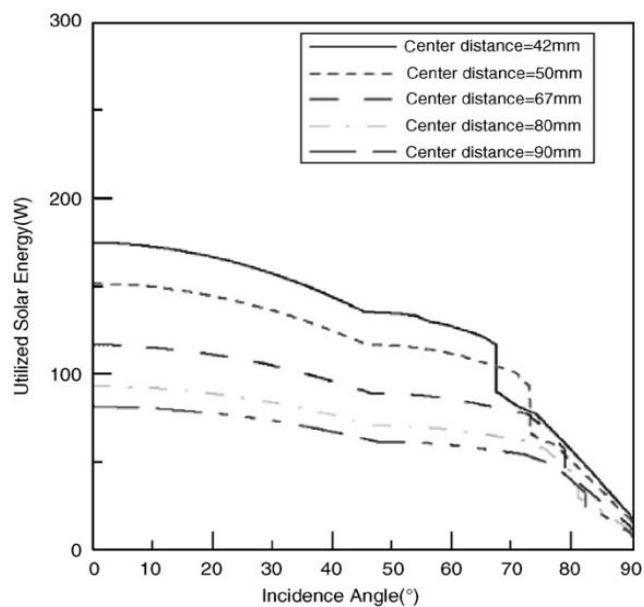


**Figure 1.7** Performance with collector tube center distance (Yong & Taebeom, 2006)

The performance of the water-in-glass systems are compared to the performance of flat plate collector with 300 liter storage volume. The water-in-glass

system is calculated in Auckland, Sydney, Melbourne, Darwin and Jakarta climatic conditions due to evaluate the performance of water-in-glass system under different conditions. The performance of water-in-glass system is evaluated by the energy saving compared to an electric water heater with a storage volume of 250 liter. Figure 1.9, shows the performance of flat plate system and two water-in-glass systems with 2.9 m<sup>2</sup> collector at 22° inclination and 220 liter of water storage tank in Sydney. The results showed that the flat plate system has an energy savings of 77%, the water-in-glass system has a saving of 70.9% and water-in-glass system with a boost tank pre-heater has a savings of 66.2%. Flat-plate collectors normally avail from separating the solar water storage tank and the boost tank pre-heater which water in storage tank improved stratification and increased collector efficiency.

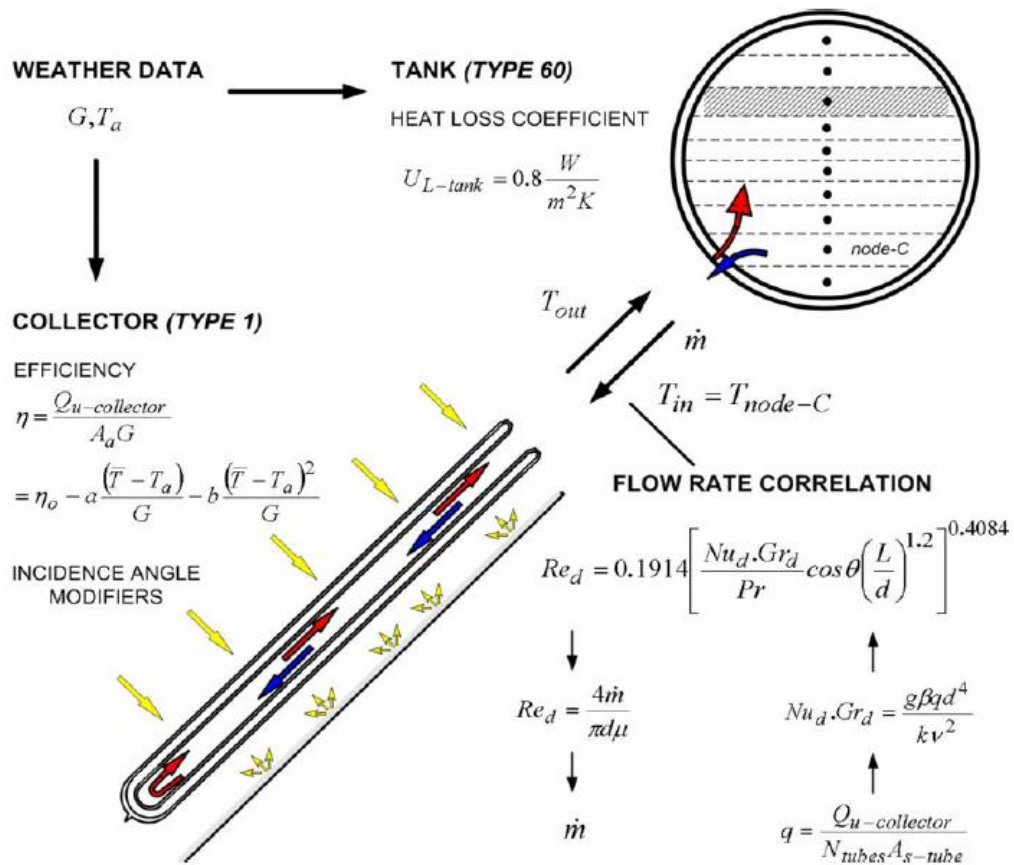


**Figure 1.8** Water-in-glass evacuated tube system (Budihardjo & Morrison, 2009)

The effect of the collector size on performance is shown in Figure 1.10. The evacuated tube systems for a small tank is 153 liter of storage tank, 2.1 m<sup>2</sup> collector

array and a 220 liter of storage tank, 2.9 m<sup>2</sup> collector array in Sydney and Melbourne are simulated at 22° inclination. The results in Sydney, the solar fraction increases from 57.5% to 70.9% when in Melbourne are 48% and 58%. In Sydney and Melbourne at 22° inclination, the collector saving for the summer months about 90% when the winter the monthly saving in Sydney is 45% and in Melbourne saving is 29%.

Azad (2008) studied of a flat plate heat pipes solar collector. The heat pipe is operating in gravity-assisted mode. The solar collector consists of six heat pipes, it made of copper tube, outside diameter is 12.7 mm (1/2 inch.) and a length is 1850 mm. The wick structure consisted of 100-mesh stainless steel fitted at the evaporator section. The heat exchanger consisted of six copper collars, an outside diameter of 20 mm and 300 mm length which fitted around the condenser section of the heat pipes. Each heat pipe is bonded to the aluminum absorber plates at 160 mm pitch are shown in Figure 1.11 and Figure 1.12.

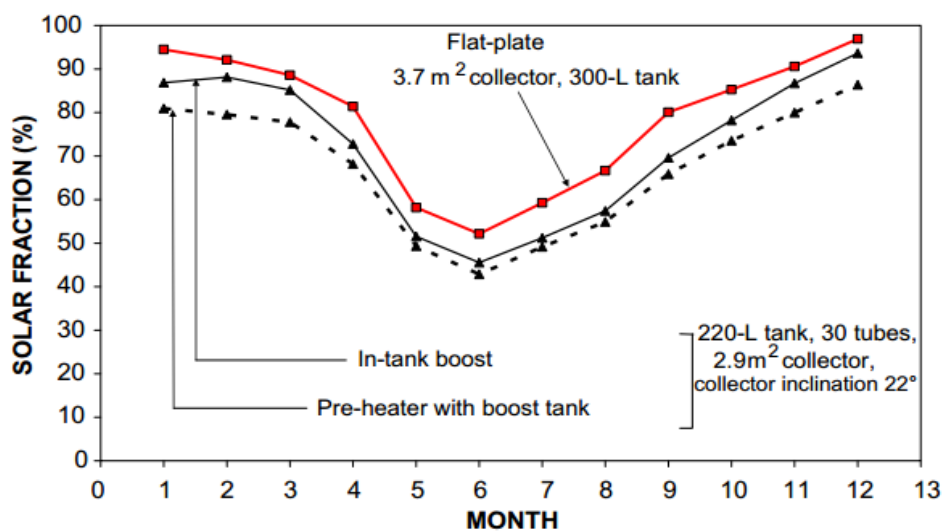


**Figure 1.9** Performance of 220 liter water-in-glass system and 300 liter flat-plate system at 22° inclination in Sydney (Budihardjo & Morrison, 2009)

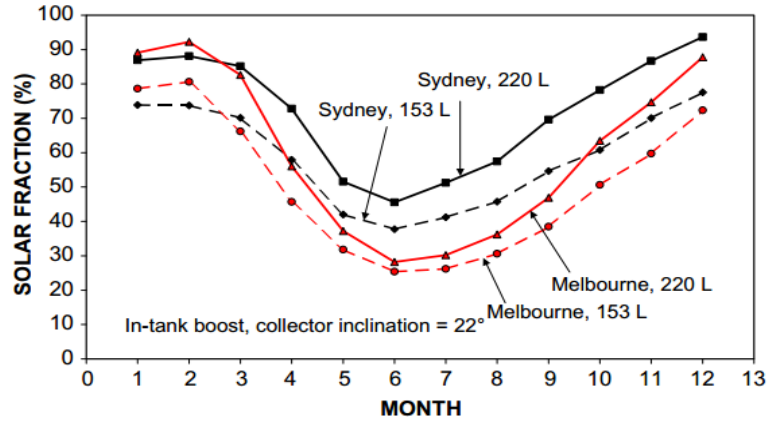


**Figure 1.10** Monthly solar fraction of different system in Sydney and Melbourne (Budihardjo & Morrison, 2009)

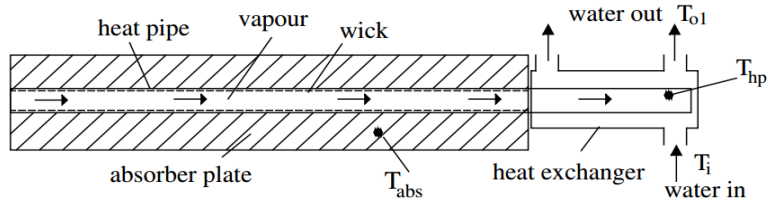


**Figure 1.11** Schematic of heat pipe with heat exchanger operation (Azad, 2008)

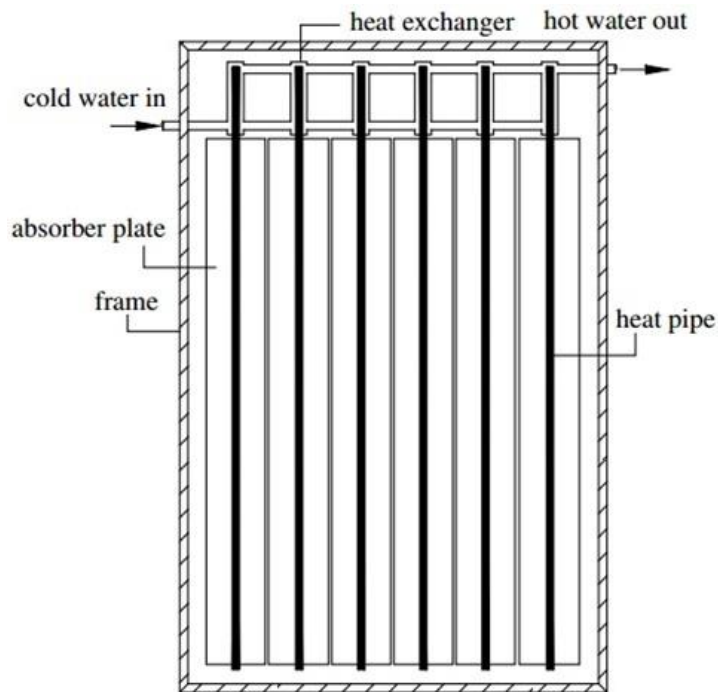


**Figure 1.12** Heat pipe solar collectors (Azad, 2008)

The outlet water temperature at the manifold is considered from the previous condenser transform into the inlet water temperature of the next condenser as shown in Figure 1.13. The collector efficiency is calculated by ASHRAE standard 93-1986. The theoretical prediction is validated accuracy from the experimental. It is found that, the temperature profiles of the heat pipe, and the hot water temperatures will affect to number of heat pipes. The water temperature slightly increases from one heat pipe to the next. The condenser temperature of the first heat pipe is 54°C and the last heat pipe is 60°C. The water temperature in the first condenser is 42°C while outlet water temperature reaches 48°C.

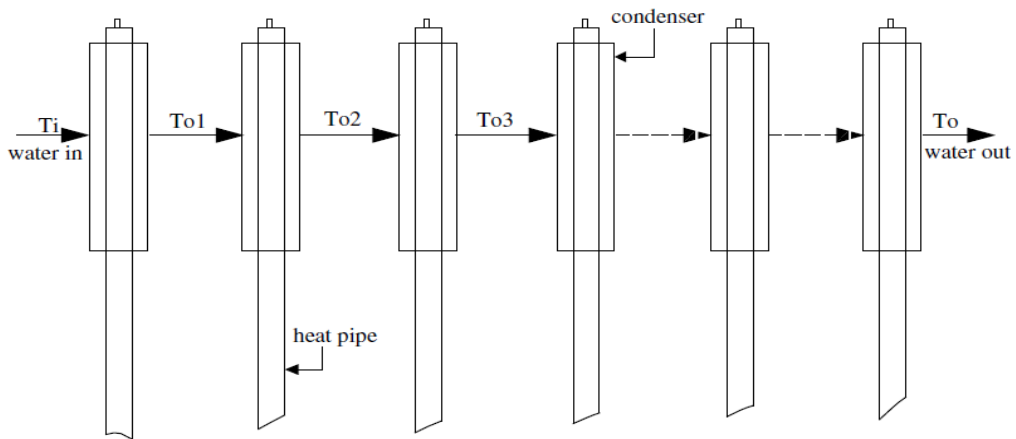


**Figure 1.13** Fluid flows in condenser (Azad, 2008)

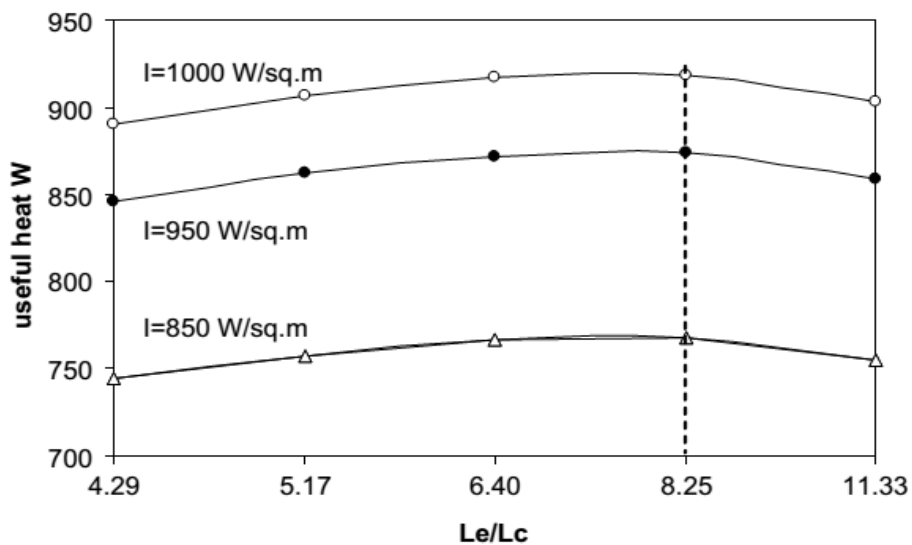


**Figure 1.14** Optimum value of  $L_e/L_c$  (Azad, 2008)

The ratio of evaporator length to condenser length ( $L_e/L_c$ ) is plotted from the useful heat as shown in Figure 1.14. The useful heat increases at the first ratio of evaporator length to condenser length reaching the maximum ratio at 8.25, and then decreases for other the ratios. With the increase of the ratio of length ( $L_e/L_c$ ), the absorber area increase will be increasing the absorbed solar and the heat loss. Whereas, the heat transfer coefficient of condenser will increase and causing to increase the heat transfer rate in the condenser. The theoretical and the experimental results are represented in Figure 1.15. It is found that, the maximum error between theoretical and experimental efficiencies occurs at 11:00 AM. From the Figure 1.15 at 11:00 AM, the theoretical efficiency is 60.3% while the experimental efficiency is 55.6% (an absolute error of 4.7%).

Chow et al. (2011) evaluated the experimental and numerical performance of the evacuated tube solar water heaters in Hong Kong. The single-phase thermosyphon and the two-phase thermosyphon are investigated. The numerical model of each system component is developed by the TRNSYS program. The theoretical and mathematical models of the open thermosyphon water-in-glass evacuated tube used of Estrada-Gasca et al., and Budihardjo and Morrison while the two-phase thermosyphon collector is developed by Farsi et al.

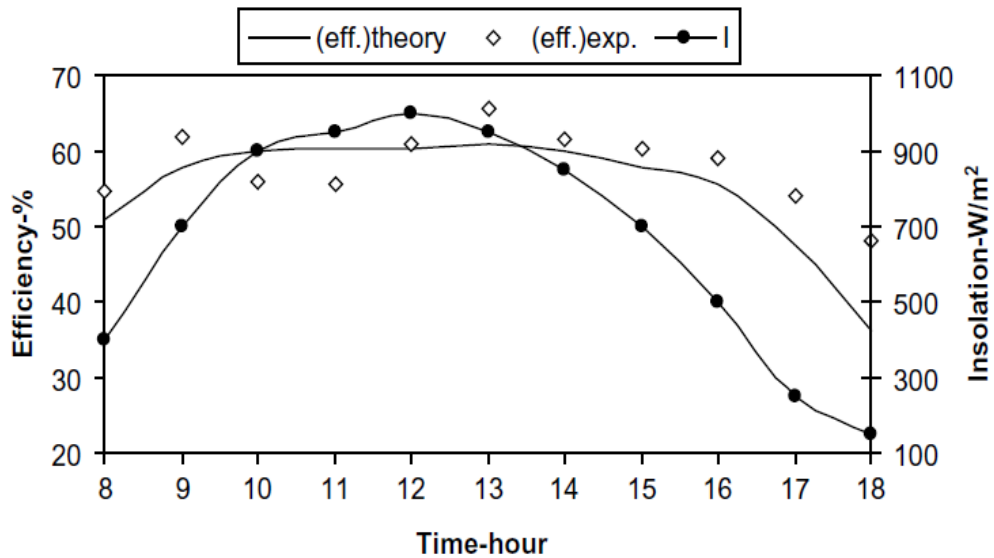


**Figure 1.15** The model efficiency and the experimental efficiency (Azad, 2008)

The model results can be validated by the experimental of the winter period test and the summer period test. The systems are assumed at the consumption rate of hot water 120 liter per day. The performances are compared with that of the flat-plate collector system. Table 1.2 shows the simulation results of the evacuated tube solar water heaters using the single-phase thermosyphon system and the two-phase thermosyphon system. It can be seen that, the annual heat accumulative the two-phase collector system is 5639 MJ, which is 12.9% higher than the 4996 MJ of the single-phase collector system. The annual savings in electrical energy for water heating are 1461 kWh and 1649 kWh, respectively.

The economics analysis compares between gas heater and electrical heater. It is found that the payback periods are about 9.40 years for two-phase thermosyphon system and 9.58 years for single-phase thermosyphon system which reference to an electrical water heater. For the gas water heater, the volumes of gas consumed are 340 m<sup>3</sup> and 384 m<sup>3</sup>. The payback periods are about 6.86 years for two-phase thermosyphon system and 7.00 years for single phase thermosyphon system which reference to gas water heater.

**Table 1.2** Performance comparisons of solar collector systems (Chow et al., 2011)

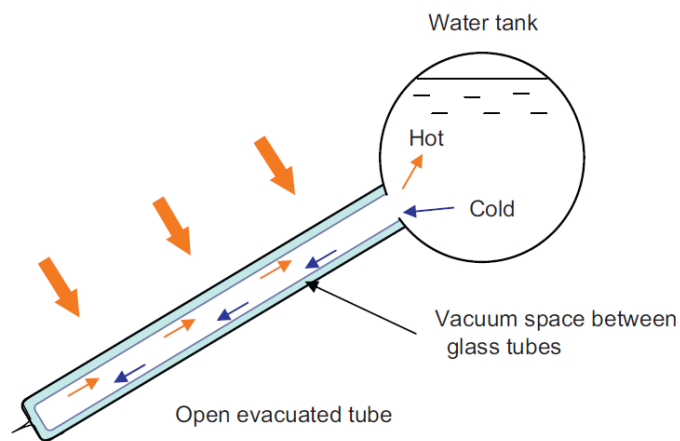
Collector type	Heat obtained (MJ/year)	Electrical energy saved (kWh/year)	Town gas saved (m <sup>3</sup> )	Payback period (year)	
				Electric heater	Gas heater
Single-phase evacuated tube	4996	1461	340	9.58	7.00
Two-phase evacuated-tube	5639	1649	384	9.40	6.86
Flat-plate	4500	1316	306	8.36	6.10

Han et al. (2008) studied the solar system composed of the parallel of vacuum tubes using an analytical model. The temperatures calculation of water from the entry to

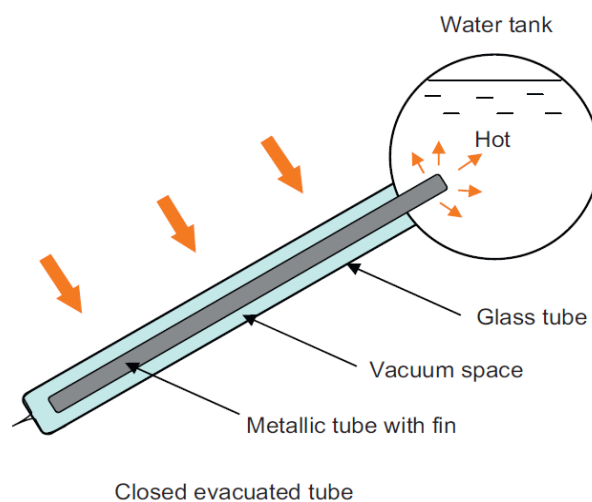
the exit under different operating conditions as shown in Figure 1.17 (a) shows differentiation of the water temperature during the inlet and outlet of the coaxial conduit and Figure 1.17 (b) shows cross section of the water temperature during the inlet and outlet. The assumptions of governing equations for analysis the thermal and hydrodynamic phenomena that take place within the vacuum tube as:

- The physical properties is constant all components.
- The uniform solar radiation is incident on the absorber surface.
- Radiation heat transfer is negligible in the coaxial fluid conduit.

Computational Fluid Dynamics (CFD) solver based on the finite volume approach has been employed.



(a) Single phase thermosyphon



Closed evacuated tube

(b) Two phase thermosyphon type



**Figure 1.16** Evacuated tube solar water heater systems (Chow et al., 2011)

The initial temperature condition assumed at 10°C same as the ambient. The effect of heat transfer of water at the inner and outer conduit is quite apparent and the hottest temperature does not necessary exist at the outlet. For the flow rate of 3 LPM, the highest water temperature is found at the outlet unless some shifts are observed at the flow rates 1 LPM and 2 LPM. For the flow rate of 1 LPM, the highest water temperature occurs halfway between the outlet and the turnaround point. The temperature of the whole tube is visualized, which during from 18°C to 55°C. The maximum temperature of absorber surface is 74°C which is the highest of all components as shown in Figure 1.18

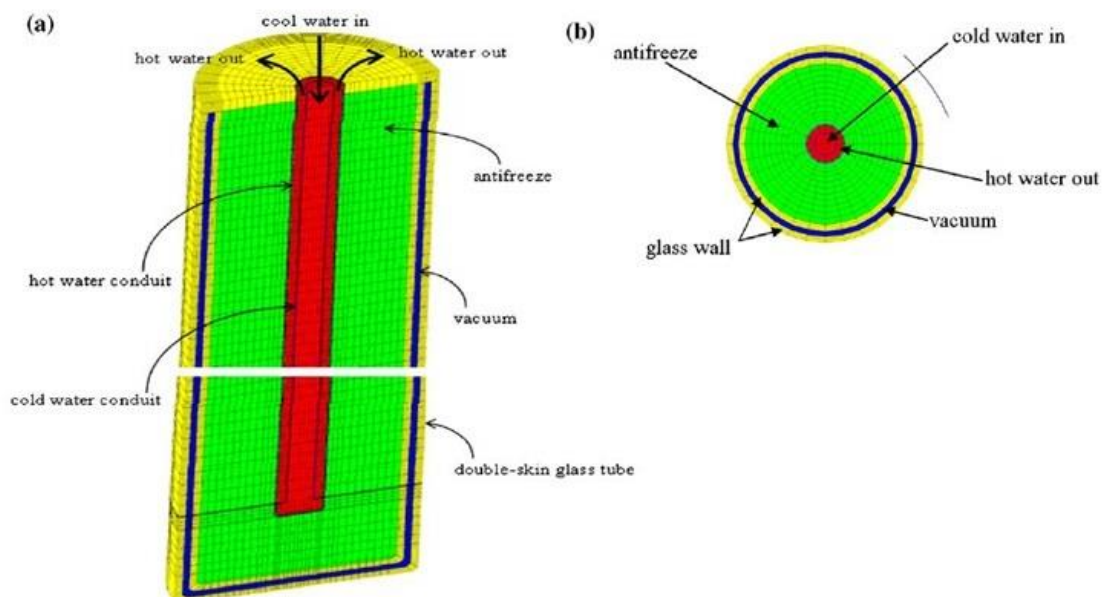


**Figure 1.17** Sectional views of the three-dimensional grid system: (a) side, (b) top (Han et al., 2010)

Shahi et al. (2010) studied three-dimensional numerical of a single-ended tube using a nano-fluid on the non-uniform heat input. The single-ended evacuated tube of water-in-glass is assumed that the sealed end of tube to be adiabatic and the tube opening to be subjected to copper–water nano-fluid as shown in Figure 1.19. In order to increase the accuracy, the Implicit Finite Volume Method by central difference are applied for solve numerically.

The governing equations of heat transfer and fluid flow considered steady-state three-dimensional, the configuration and taking into account the following assumptions: (a) Incompressible and laminar flow. (b) Newtonian behavior. (c) Viscous dissipation in the energy equation is negligible. (d) Except for the density the properties fluid are taken to be constant. (e) The Boussinesq approximation is valid for buoyancy force.

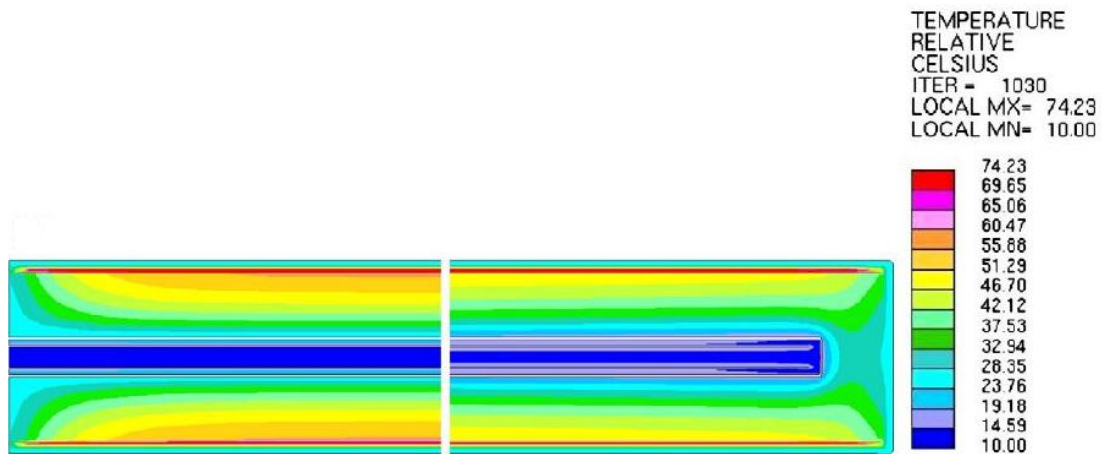


**Figure 1.18** Development of flow field and temperature distribution top  
(Han et al., 2010)

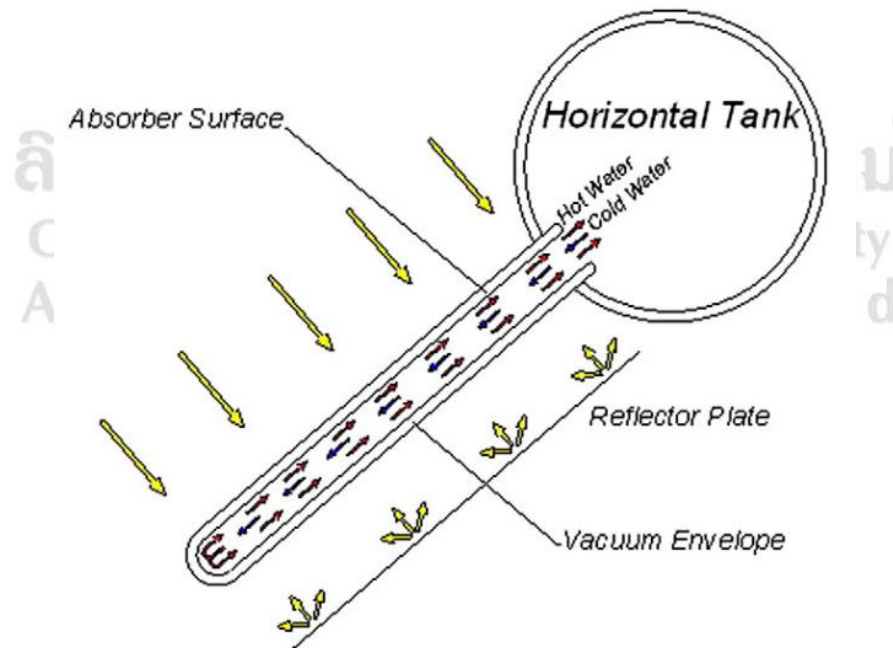


**Figure 1.19** Schematic of water-in-glass solar water heater (Shahi et al., 2010)

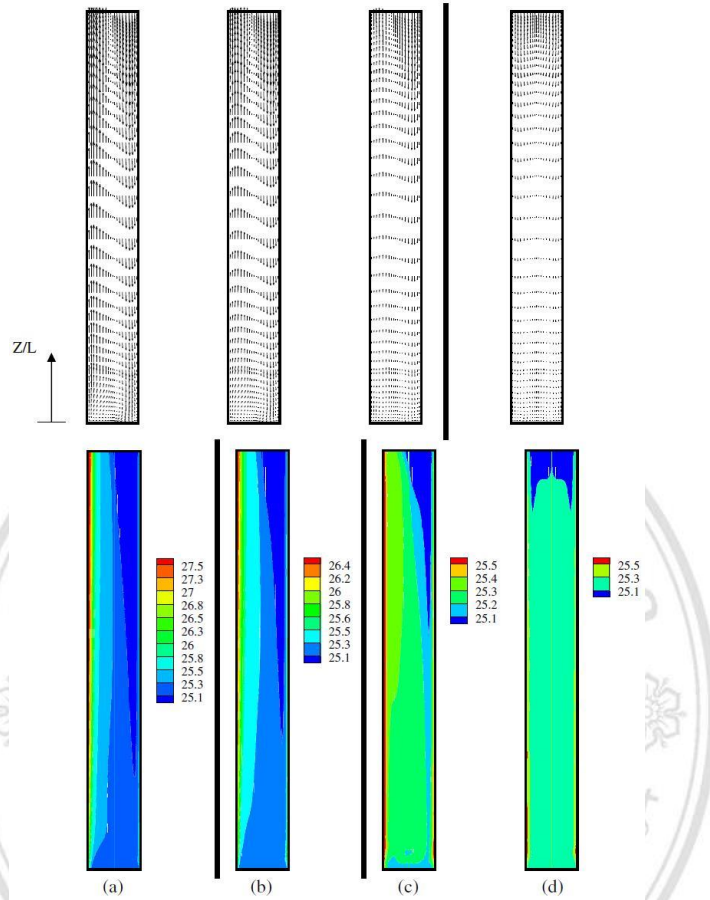


**Figure 1.20** Velocity vector and temperature distribution on different longitudinal sections for the inclination angle of (a) 15° (b) 35° (c) 55° (d) 75° (Shahi et al., 2010)

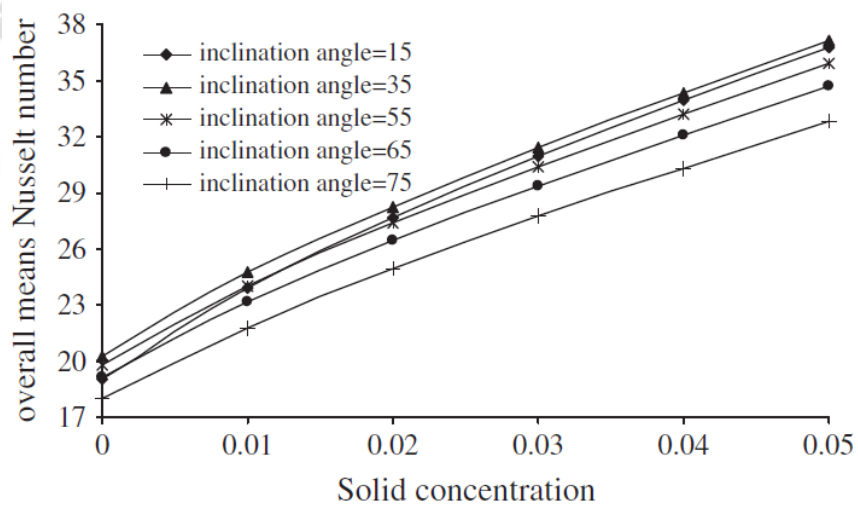


**Figure 1.21** The variation of the Nusselt number (Shahi et al., 2010)

Velocity vectors of water-in-glass on the longitudinal sections (a, b, c and d) as shown in Figure 1.20. The effect of the inclination angle showed that the maximum Nusselt number is occurred at  $\gamma=35^\circ$ , while the maximum mass flow rate is increasing function of the inclination angle as shown in Figure 1.21.

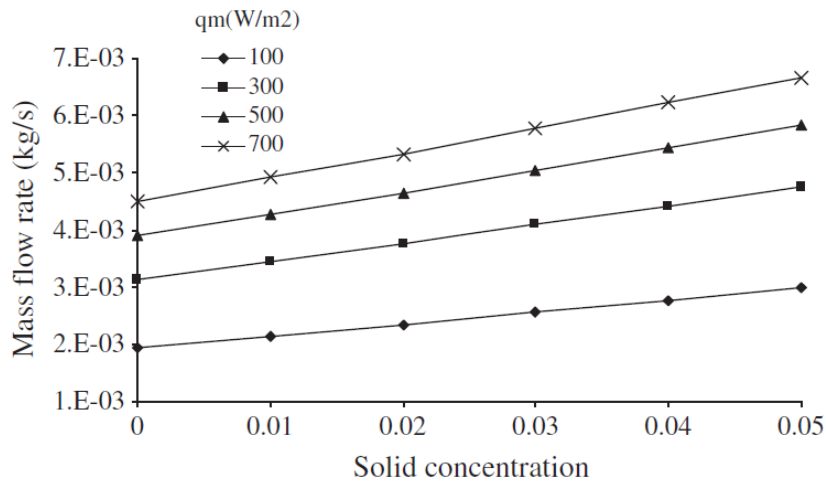


**Figure 1.22** The variation of the mass flow rate versus solid concentration for different heat fluxes at  $\gamma=35^\circ$  (Shahi et al., 2010)

Figure 1.22 shows the effect of mass flow rate on the variation of the Nusselt number. The temperature increases by increasing the heat input. Because the nanoparticles enhance the effective thermal conductivity and the energy is more transferred between fluid layers. At heat input  $700 \text{ W/m}^2$ , the mass flow rate increases about 47.9% compare to the pure fluid. The nano-fluid has more effect at the high heat input. So that with 5% increase of the solid, the Nusselt number enhances 62% at heat input  $100 \text{ W/m}^2$  and about more than 100% at heat input  $700 \text{ W/m}^2$ .

Sato et al. (2012) studies the transient analysis of an evacuated tube collector and developed geometry. For the thermal analysis comprise solved by Navier-Stokes and energy equation. Computational Fluid Dynamics (CFD) and Computational Heat Transfer (CHT) are employed to model. The cross-section views are presented in Figure 1.23. The initial temperature of the models is set as 300 K, the uniform heat flux on the surface is  $500 \text{ W/m}^2$ , and the different tilt angles are investigated with  $30^\circ$ ,  $45^\circ$  and  $60^\circ$ .

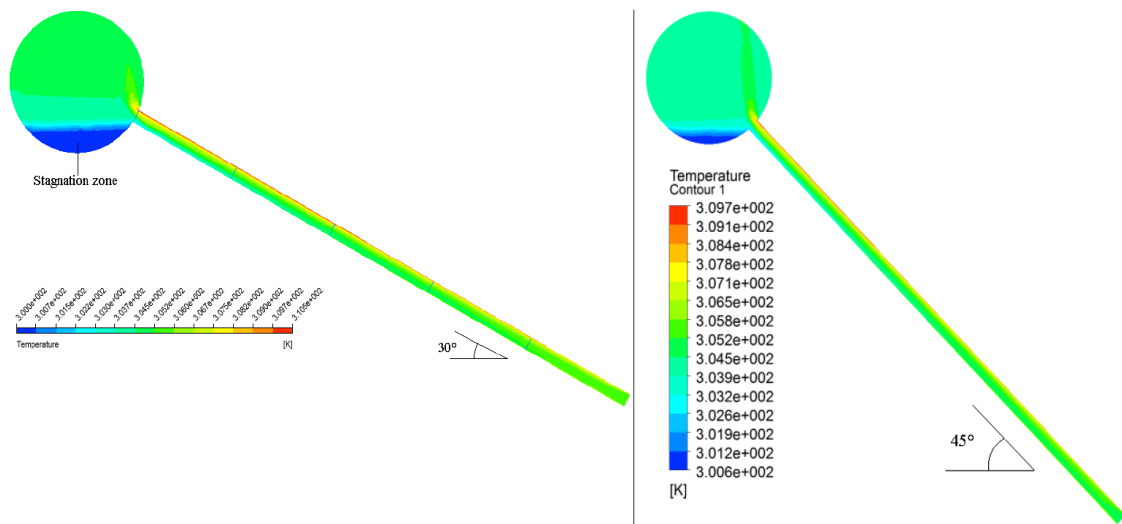


**Figure 1.23** Temperature distribution of the conventional solar collector with tilt angle of  $30^\circ$  and  $45^\circ$  (Sato et al., 2012)

The result, the water temperature profile and thermal stratification of a conventional solar collector with  $30^\circ$  tilt angle and  $45^\circ$  tilt angle as shown in Figure 1.23. At  $45^\circ$  tilt angle, the stagnation area still appears but with less intensity as seen at  $30^\circ$ . The recirculation zone, the water velocity increases by increasing of solar collector tilt angles. This occurs based on the buoyancy to the higher tilt angles.

Comparing the thermal performance of the model with inferior connection, subjected to different tilt angles, the results showed a small temperatures difference between the developments achieved in each analysis. The temperatures are measured at the tank and tube connection, the temperature for the three tilt angles as shown in Figure 1.24, the conventional collector showed higher temperature values. At the same time, the two collectors presented same behavior in temperature evolution, but the geometry with inferior connection obtained temperature magnitudes higher than the other model.

From the previous literature, the optimal design of evacuated tube solar water heater system using two-phase thermosyphon has not been studied. Consequently, this research, computer program and Finite Difference Method (FDM) are employed to predict the optimal variable parameter for design and construct the prototype solar water heater system. The mathematical models data are validated by the experimental data.

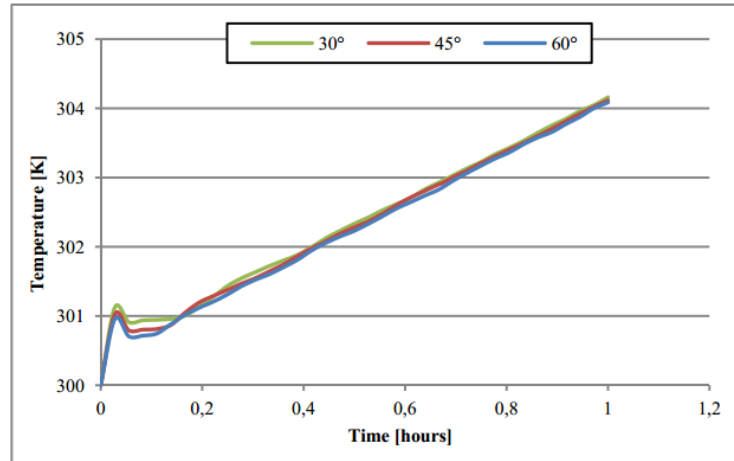


**Figure 1.24** Temperature profiles of different tilt angles (Sato et al., 2012)

### 1.3 Objective of this study

1.3.1 To develop a mathematical model of single evacuated tube using thermal resistance method and Finite Difference Method (FDM).

1.3.2 To analyze the optimal design for number of evacuated tubes and two-phase thermosyphon dimensions of solar water heater system from mathematical model data by using the thermoeconomics method.

1.3.3 To design, construct and test the appropriate solar water heater system, comparison between experimental data, as well as mathematical model data will also be investigated.

1.3.4 To analyze the economics of solar water heater system compared to the electric water heater.

### 1.4 Significance

1.4.1 The mathematical models can help predicting hot water temperature, heat rate of water, and thermal efficiency of solar water heater system.

1.4.2 An appropriate dimensions of two-phase thermosyphon can be applied to the solar water heat system.

## **1.5 Scope of this study**

The scope of this study can be divided into two parts.

### **1.5.1 Mathematical model**

1.5.1.1 Establishing the mathematical models of the evacuated tube solar water heater using thermal resistance method and Finite Difference Method.

1.5.1.2 The evacuated tube is a coaxial double-layer tube with 58 mm of outer tube diameter, 47 mm of inner tube diameter and 1800 mm of total length.

1.5.1.3 A thermosyphon is made of copper tube.

1.5.1.4 A thermosyphon is used R141b as the working fluid and filling ratio of 70 % of the evaporator section volume.

1.5.1.5 The water storage tank volume is 50 liter of the single evacuated tube and 100 liters of evacuated tube solar water heater system.

1.5.1.6 A water flow rate is 0.03 kg/s (Nada et al., 2004).

1.5.1.7 The solar intensity and ambient air temperature data of Chiang Mai province, Thailand are used as the input of modeling program.

### **1.5.2 Experimental work**

There are two experimental as follows:

1.5.2.1 The experiment is conducted by using the single evacuated tube with refrigerant thermosyphon and industrial thermosyphon. The refrigerant thermosyphon is filled R141b as the filling ratio about 70% of evaporator volume while the working fluid of industrial thermosyphon is filled by the water and copper powder. Both thermosyphons are tested under tilt angle at 18° and facing south, water flow rate is 0.03 kg/s, 50 liters of water storage tank and identical environmental. The solar intensity and ambient air temperature are inputted to the modeling program. The mathematical model results can be verified by the experimental results. After that, the heat rate of water on net saving from the mathematical program is investigated for determining the optimal of thermosyphon dimensional and number of evacuated tube, under the condition that hot

water in storage tank over 65°C. The optimal parameter is selected for the design, construct and test in the experiment.

1.5.2.2 For the testing of the evacuated tube solar water heater system, the system consisted of optimal thermosyphon dimensions, the number of evacuated tube, and a hot water storage tank of 100 liters. The system is tested under tilt angle at 18° and facing south, 0.03 kg/s of water flow rate. For the mathematical models, the solar intensity, ambient air temperature and wind velocity are inputted to the modeling program. The mathematical model results are verified with the experimental results.

## **1.6 Benefit of this study**

1.6.1 The mathematical models of the evacuated tube solar water heater system with two-phase thermosyphon are established to predict heat transfer rate, hot water temperature, and thermosyphon dimensions.

1.6.2 The prototype of the evacuated tube solar water heater system with two-phase thermosyphon leads to the development for applied to domestic or industry operation.

